Sucrose Signaling Regulates Anthocyanin Biosynthesis Through a MAPK Cascade in *Arabidopsis thaliana*

Lai-Sheng Meng,*[,1,2] Meng-Ke Xu,*[,2] Wen Wan,*[,2] Fei Yu,* Cong Li,[†] Jing-Yi Wang,* Zhi-Qin Wei,* Meng-Jiao Lv,* Xiao-Ying Cao,* Zong-Yun Li,*[,1] and Ji-Hong Jiang*

*The Key Laboratory for Biotechnology on Medicinal Plants of Jiangsu Province, School of Life Science, Jiangsu Normal University, Xuzhou, 221116, People's Republic of China and [†]Public Technical Service Center, Kunming Institute of Zoology, Chinese Academy of Sciences, Yunnan, 650223, People's Republic of China

ORCID ID: 0000-0002-8844-4356 (L.-S.M.)

ABSTRACT Anthocyanin accumulation specifically depends on sucrose (Suc) signaling. However, the molecular basis of this process remains unknown. In this study, *in vitro* pull-down assays identified ETHYLENE-INSENSITIVE3 (EIN3), a component of both sugar signaling or/and metabolism. This protein interacted with YDA, and the physiological relevance of this interaction was confirmed by *in planta* co-immunoprecipitation, yeast two-hybrid (Y2H) assay, and bimolecular fluorescence complementation. *Ethylene insensitive3-like 1* (*eil1*) *ein3* double-mutant seedlings, but not *ein3-1* seedlings, showed anthocyanin accumulation. Furthermore, *ein3-1* suppressed anthocyanin accumulation in *yda-1* plants. Thus, *EMB71/YDA-EIN3-EIL1* may form a sugar-mediated gene cascade integral to the regulation of anthocyanin accumulation. Moreover, the *EMB71/YDA-EIN3-EIL1* gene cascade module directly targeted the promoter of *Transparent Testa 8* (*TT8*) by direct EIN3 binding. Collectively, our data inferred a molecular model where the signaling cascade of the YDA-EIN3-TT8 appeared to target *TT8* via EIN3, thereby modulating Suc signaling–mediated anthocyanin accumulation.

KEYWORDS EMB71/YODA(YDA); anthocyanin biosynthesis; ETHYLENE-INSENSITIVE3 (EIN3); TT8; sugar signal or/and metabolism; ethylene signal

ANTHOCYANINS are a class of flavonoids widely found in plants and play important roles in many of physiological processes, including functioning as photoprotective screens in vegetative tissue, visual attractors in pollination, antimicrobial agents, and feeding deterrents in the defense response (Winkel-Shirley 2001).

Anthocyanin accumulation is stimulated via many endogenous signals, for example, sucrose (Teng *et al.* 2005), auxin, abscisic acid (ABA) (Jeong *et al.* 2004, 2010; Hoth *et al.* 2010), gibberellin (Weiss *et al.* 1995), cytokinin (Deikman and Hammer 1995), jasmonates (Qi *et al.* 2011), and ethylene (Morgan and Drew 1997). Further, the synthesis of these molecules is also induced by a series of environmental stresses, including attempted microbial infection, ultraviolet irradiation, insect attack, wounding, nutrient depletion, and drought (Qi *et al.* 2011).

MYB/bHLH/TTG1 (MBW) components are thought to regulate anthocyanin biosynthesis in a spatiotemporal manner (Teng *et al.* 2005). In *Arabidopsis thaliana*, the WD-repeat protein Transparent Testa Glabra 1 (TTG1) (Walker *et al.* 1999) recruits basic helix-loop-helix (bHLH) transcription factors (Toledo-Ortiz *et al.* 2003); for example, Transparent Testa 8 (TT8) (Nesi *et al.* 2000; Baudry *et al.* 2006), Glabra 3 (GL3) (Payne *et al.* 2000), or Enhancer of Glabra 3 (EGL3) (Zhang *et al.* 2003). Further, R2R3 MYB transcription factors (MYB113, MYB90, MYB114, or MYB75) (Borevitz *et al.* 2000; Stracke *et al.* 2001, 2007; Zimmermann *et al.* 2004; Gonzalez *et al.* 2008; Rowan *et al.* 2009) can also be recruited. Collectively, these proteins form the WD-repeat/bHLH/MYB component complex. This complex regulates anthocyanin biosynthesis via promoting the expression of late anthocyanin biosynthetic genes, including leucoanthocyanidin dioxygenase, NADPH-dependent dihydroflavonol reductase (DFR), and UDP-Glc:flavonoid 3-Oglucosyltransferase (UF3GT) (Dooner *et al.* 1991; Kubasek *et al.* 1992; Shirley *et al.* 1995; Gonzalez *et al.* 2008).

doi: https://doi.org/10.1534/genetics.118.301470
Manuscript received June 30, 2018; accepted for publication August 6, 2018; published Early Online August 16, 2018.
Supplemental material available at Figshare: https://doi.org/10.6084/m9.figshare.6974570.
[1]Corresponding authors: Jiangsu Normal University, 101 Shanghai Rd., Tongshan Region, Xuzhou City 221116, China. E-mail: menglsh@jsnu.edu.cn; zongyunli@jsnu.edu.cn
[2]These authors contributed equally to this work.

Sucrose (Suc) is a well-characterized endogenous developmental signal. Sugars (*e.g.*, Suc) play dual functions as transported carbohydrates in vascular plants and as signal molecules that regulate gene expression and plant development. Sugar-mediated signals indicate carbohydrate availability and regulate metabolism by coordinating sugar production and mobilization with sugar usage and storage (Baier *et al.* 2004). Anthocyanin biosynthesis is modulated by changes in Suc concentrations and the sugar-dependent upregulation of the anthocyanin synthesis pathway is Suc-specific (Solfanelli *et al.* 2006; Jeong *et al.* 2010). The *Arabidopsis pho3* mutant is defective in *Suc transporter 2* (*SUC2*) function. *SUC2* encodes a phloem-loading Suc-proton symporter, enabling accumulation of soluble sugars; thus, *pho3* plants exhibit growth retardation and also anthocyanin accumulation (Lloyd and Zakhleniuk 2004). Microarray analysis of mature leaves from *pho3* plants revealed an increased expression of *PRODUCTION OF ANTHOCYANIN PIGMENT 1* (*PAP1*), *PRODUCTION OF ANTHOCYANIN PIGMENT 2* (*PAP2*), and *TT8* transcription factors, as well as of genes encoding anthocyanin biosynthesis enzymes, implying that sugar is a trigger of anthocyanin biosynthesis *in vivo* (Lloyd and Zakhleniuk 2004).

YODA (YDA), a mitogen-activated protein kinase kinase kinase (MAPKKK), is a member of the MEKK subfamily of the MEKK1/Ste11/Bck1 class of MAPKKKs and is a key component of the regulatory pathways for both embryo and stomatal development (Bergmann *et al.* 2004; Lukowitz *et al.* 2004). Current reports indicate that YDA is involved in the regulation of floral patterning (Bemis *et al.* 2013), drought tolerance (Meng and Yao 2015), anthocyanin accumulation (Meng *et al.* 2016), the accumulation of reactive oxygen intermediates, and cell death development (Li *et al.* 2015). A previously reported microarray analysis of *yda* mutants (Lukowitz *et al.* 2004) indicated that only 14 out of 8000 genes had changes in expression levels of at least twofold; this gene set included those associated with sugar metabolism or carbohydrate metabolic process (AT5G57550, AT2G43570, and AT4G15760), and cell wall synthesis (At2g45220). Thus, over half were related to sugar metabolism and/or sugar signaling. A further microarray study of *yda* plants revealed that over 11% of upregulated genes were involved in cell wall differentiation (Bergmann *et al.* 2004), consistent with the cell walls of differentiated epidermal cells being extensively reinforced. Collectively, these results suggest that YDA might be involved in sugar metabolism and/or sugar signaling. However, to date, there are no reports providing data to support this hypothesis.

While there are currently many different signaling pathways identified as influencing anthocyanin biosynthesis in *Arabidopsis*, it is fully unknown how these signal pathways are integrated. Here, we found that loss of YDA function enhanced anthocyanin accumulation and conveyed insensitivity to sugar signaling or/and metabolism. Further, YDA was found to interact with EIN3 *in vitro* and *in vivo* put-down, which were confirmed by yeast two-hybrid (YH2) and bimolecular fluorescence complementation (BiFC). Thus, *EMB71/YDA-EIN3-EIL1* may form a sugar-regulated gene cascade that controls anthocyanin accumulation. Interestingly, the YDA-EIN3/EIL1 complex directly targets to the *TT8* promoter for transcriptional repression, thereby negatively regulating anthocyanin biosynthesis. Our data suggests this is mediated via direct EIN3 binding to the *TT8* promoter, repressing the expression of this transcriptional activator. Collectively, our data suggests that the *YDA-EIN3-TT8* gene cascade modules may target the *TT8* promoter by direct EIN3 binding, regulating anthocyanin biosynthesis.

Materials and Methods

Plant materials and growth conditions

The *yda-1* and *yda-2* (Lukowitz *et al.* 2004), *ein3-1*, *eil1-3*, *ctr1-1* and *ein3/eil1* (An *et al.* 2010) mutants, and the estradiol-inducible *EIN3–FLAG* transgene (An *et al.* 2010) within a Col-0 background were all described previously.

The *yda-1*, *yda-2*, *ctr1-1*, *tt8-1*, and *emb71* mutants were obtained from the *Arabidopsis* Biological Resource Center (Ohio State University). The EIN3-FLAG, *eil1-3*, *ein3-1*, and *ein3/eil1* seeds were kindly provided by Prof H. W. Guo (Peking University, China). The *pHB-YDA:GFP* plasmid was kindly provided by Prof. H. Q Yang (Shanghai JiaoTong University, China). The *pHB-35Spro-YDA:GFP* transgene is driven by the *35S* promoter (Bergmann *et al.* 2004; Kang *et al.* 2009).

The *yda-1/+ein3* mutant was obtained from F2 seedlings of a *yda-1/+ein3-1* cross that had shortened roots (Lukowitz *et al.* 2004) and had lengthened hypocotyls and roots on solid Murashige and Skoog Medium (MS) medium with 6.0 μm l-aminocyclopropane-l-carboxylic acid (ACC) (An *et al.* 2010). The *yda/ein3* mutant was identified from offspring of *yda-1/+ein3-1* that had clustered stomata on the cotyledon in the dark (Kang *et al.* 2009), and then homozygous lines were identified through PCR-based genotyping for *ein3-1*. Primers for *ein3-1* were described previously (An *et al.* 2010). Similarly, we obtained *ein3/tt8 and ein3/eil1/tt8* mutants. The method of double-mutant construction has been described by Kang *et al.* (2009).

For simultaneous germination, seeds were treated with jarovization at 4° overnight and then sown on solid MS medium supplemented with 1% sucrose (pH 5.8) and 0.8% agar (Meng and Yao 2015). Seedlings grown on agar were maintained in a growth room under 16:8 hr of light/dark cycle with cool white fluorescent light at 21 ± 2° (Meng and Yao 2015). Plants grown in soil were maintained in a controlled environment growth chamber under 16:8 hr light/dark cycle with cool white fluorescent light at 21 ± 2° (Meng and Yao 2015).

Confocal laser scanning microscope for GFP or YFP imaging

Subcellular localization of relative fusion protein/gene expression was assayed within the abaxial epidermis of cotyledons in 1-week-old transgenic plants harboring the relative vector. An Olympus IX-70 microscope (http://www.

olympus-global.com/) was used to detect GFP or YFP expression. The sections were photographed under a confocal laser scanning microscope.

Y2H assays

The Y2H analysis was carried out using a GAL4-based Y2H system from MatchmakerGold Systems (Clontech, Palo Alto, CA). The full-length complementary DNA (cDNA) of YDA was cut with *Not*I and *Sfi*I and ligated into *pGBKT7* to construct a bait plasmid. The full-length cDNA of EIN3 was cloned into *pGADT7* to construct prey plasmid using *Bam*HI and *Xho*I. Primers for pGADT7+EIN3 were YTH-EIN3-F: CGC GGA TCC ATG ATG TTT AAT GAG ATG GGA (*Bam*H), and YTH-EIN3-R: CCG CTC GAG TTA GAA CCA TAT GGA TAC ATC (*Xho*I); and primers for pGBKT7-YDA were YTH-YDA-F: ATG GCC ATG GAG GCC ATG CCT TGG TGG AGT AAA TCA (*Sfi*I), and YTH-YDA-R: ATA AGA ATG CGG CCG CTT AGG GTC CTC TGT TTG TTG (*Not*I). To test the interaction, the bait plasmid and the prey plasmid were cotransformed into yeast strain Y2H Gold (Clontech) and yeast cells containing both vectors were selected using synthetic dropout (SD)/-Leu/-Trp (DDO) medium. The transformants were assayed by plating the transformed cells onto the SD/-Ade/-His/-Leu/-Trp selective medium (QDO) and QDO/Aba/X-α-Gal selective medium using at least 10 independent colonies for the β-galactosidase test. Serial dilutions of cotransformed yeast cells were used to measure the strength of the interaction.

BiFC assays

To perform this assay, *pBI121-YFPC* was produced by using YFPC-F (K): 5′ CGG GGT ACC TAC CCA TAC GAT GTT CCA GAT T 3′ *Kpn*I and YFPC-R (S): 5′ CGA GCT CTT ACT TGT ACA GCT CGT CCA TG 3′ *Sca*I; and *pBI121-YFPN* was produced by using YFPN-F (K): 5′ CGG GGT ACC GAG CAA AAG TTG ATT TCT GAG G 3′ *Kpn*I and YFPN-R (S): 5′ CGA GCT CTT AGG CCA TGA TAT AGA CGT TGT 3′ *Sca*I; and *pBI121-YFPN-EIN*3 was produced by using YTH-EIN3-F: CGC GGA TCC ATG ATG TTT AAT GAG ATG GGA *Bam*HI and YTH-EIN3-R: CCG CTC GAG TTA GAA CCA TAT GGA TAC ATC *Xho*I; and *pBI121-YFPC-YDA* was produced by using BIFC-YDA-F: GGG GTA CCA TGG AAA AAA GGG AGA TTG C *Kpn*I and BIFC-YDA-R: CCG CTC GAG AAA GCA TGA TCC AAA AGC TG *Xho*I. To perform the BiFC assays, leaf blades of *Nicotiana benthamiana* were transformed transiently with *Agrobacterium tumefaciens*. The *Agrobacterium* strains containing the BiFC constructs were grown on OD = 1.0, spun down, and then resuspended in infiltration buffer (10 mM 2-(4-Morpholino) ethanesulfonic acid (MES), 10 mM MgCl2, and 100 mM acetosyringone) to OD = 1.3. Then, they were incubated on a shaker at room temperature for 3–4 hr. Strains containing the two assayed constructs were mixed and then injected into the middle of leaf blades. Leaf blades were imaged via laser scanning confocal microscope and DIC to 3 days after injection. Every interacting pair was tested for two repeated experiments.

Assaying seedling response to high concentration of sugar and ethylene

The use of 1 and 5% mannitol, sucrose and glucose was performed, as has been shown by Meng *et al.* (2016). Ethylene, ACC, and AgNO3 conditions were described by Jeong *et al.* (2010).

Assay of sugar metabolites

Twelve-day-old seedlings were ground in liquid nitrogen, and then the powder was isolated with 1 ml of 80% ethanol for 1 hr. These extracts were centrifuged with 12,000 × *g* for 10–15 min. The supernatant along with ethanol buffer was transferred to a fresh tube and evaporated under vacuum for dryness for 40–60 min. The residues were then redissolved in 600 μl of double-distilled water and kept at 70° for 10–15 min.

Using chloroform:isoamyl alcohol (24:1, v/v), the above aqueous fraction was extracted twice to three times before HPLC analysis. Sugars were quantified and identified via chromatography on an Agilent carbohydrate column and tested with a refractive index detector (Altex 156; Altex Scientific Inc.). Concentrations were measured from peak heights using sucrose, fructose, and glucose (20 mg/ml) as standard samples. These experiments were repeated at least twice, with similar results.

Measurement of anthocyanins

For anthocyanin extraction, the given samples were placed in 50 ml of 1% HCl in methanol (v/v) and then incubated overnight in the dark at 4° with gentle shaking. After this process, 300 ml of water and 300 ml of chloroform were added and mixed to the extract. After centrifugation at 12,000 rpm for 2 min, the absorbance of the supernatant was measured at 530 and 657 nm and the concentration of anthocyanin was determined by using A530- 0.25A657 (Rabino and Mancinelli 1986). These experiments were repeated at least two times with similar results.

Quantitative PCR

Total RNA was extracted from tissues indicated in the figures by the TRIzol reagent (Invitrogen, Carlsbad, CA), as has been described by Meng and Yao (2015) and Meng *et al.* (2018). SYBR green was used to monitor the kinetics of PCR product in real-time RT-PCR, as has been described by Meng and Yao (2015). Primers of *TT8*, *PAP2*, and *MYBL2* have been described by Jeong *et al.* (2010). These experiments were repeated at least two times, with similar results.

Protein expression and purification

The plasmids *pGEX-5X-1* (for *EIN3*, *CINV2*, *SUC1*, and *HXK1*) and *pET28a* (for *YDA*) was utilized. The coding sequence of *YDA* was amplified by the primer pair (5′-GC-GGCCTTTTTG GCC-ATGCCTTGGTGGAGTAAATCAA-3′ and 5′-ATAAGAAT-GCGGCCGC-TTAGGGTCCTCTGTTTGTTGAT-3′) and cloned into the *Not*1 and *Sfi*1 restriction sites of *pET28a*. The coding sequence of *CINV2* was amplified by the primer pair (5′-CG

GGATCC-TGGAGGAAGGTCATAAAGAAC-3′ and 5-GGAATTC TCAGCAAGTCCATGAAGCAGAT-3′) and cloned into the *Bam*1H and *Eco*R1 restriction sites of *pGEX-5X-1*.

The coding sequence of *EIN3* was amplified by the primer pair (5′-GGATCC ATGATGTTTA ATGAGATGGG-3′ and 5′-CT CGAGTGCTCTGTTTGGGAT-3′) and cloned into the *Bam*1H and *Xho*I restriction sites of *pGEX-5X-1*. The coding sequence of *HXK1* was amplified by the primer pair (5′-GGATC CATGGGTAAAGTAGCTGTTGGA-3′ and 5′-CTCGAGTTAA GAGTCTTCAAGGTAGAG-3′) and cloned into the *Bam*1H and *Xho*I restriction sites of *pGEX-5X-1*. The coding sequence of *SUC1* was amplified by the primer pair (5′-GAATTC ATGG GAGCCTATGAAACAGA-3′ and 5′-CCCGGGCTAGTGGAATC CTCCCATGGT-3′) and cloned into the *Bam*1H and *Sma*I restriction sites of *pGEX-5X-1*. Recombinant glutathione S-transferase binding protein (GST)–tagged EIN3, CINV2, HXK1, and SUC1 and recombinant histidine (HIS) binding protein–tagged YDA were extracted from transformed *Escherichia coli* (*Rosetta2*) after 10 hr of incubation at 16°, following induction with 10 μM isopropyl ß-D-1-thiogalactopyranoside. These recombinant proteins were purified using HIS or GST agarose affinity, respectively.

Chromatin immunoprecipitation PCR

The transgenic lines containing estradiol-inducible *EIN3-FLAG* and *35S:EIN3-GFP* were utilized. Chromatin immunoprecipitation (ChIP) was performed with seedlings (Meng 2015). Leaf blades were incubated in buffer [1.0 mM PMSF, 0.5 M sucrose, 1 mM ethylenediaminetetraacetic acid (EDTA), 10–12 mM Tris (pH 8.0), and 1% formaldehyde] under vacuum for 15–20 min for cross-linking the chromatin. Then, 0.1 M Gly was placed in the mixture, incubating for an additional 5 min for terminating the reaction. Leaf blades were placed and ground in liquid nitrogen and resuspended to lysis buffer [150 mM NaCl,1 mMEDTA, 0.1% SDS, 0.1% deoxycholate, 50 mM HEPES (pH 7.5), 1% Triton X-100, 10 mM sodium butyrate, 1 mM PMSF, and 13 complete protease inhibitor; Roche]. Chromatin was sheared to ∼200–500 bp fragments via sonication followed by centrifuged. At 4°, supernatants were precleared under protein G agarose beads for 1–1.5 hr. Input material (supernatant containing chromatin) was used for immunoprecipitation with anti-FLAG antibody and anti-GFP antibody. Anti-FLAG antibody and anti-GFP antibody bound to EIN3-FLAG or GFP-chromatin complexes was incubated with protein G agarose beads for 1–1.5 hr at 4–6°, and then washed several times and eluted with elution buffer. Input and immunoprecipitated chromatin were uncross-linked for 6 hr at 6° with 5 M NaCl. Immunoprecipitated chromatin and input were used for PCR analysis The ChIP DNA products were analyzed PCR using five pairs of primers that were synthesized to amplify ∼300 bp DNA fragments in the promoter region of *TT8*, *PAP2*, and *MYBL2*. Primer sequences (F-5′-atgttcagtttagctt tagttcg-3′ and R-5′-aaacttaaatatataacttgaatttg-3′)-*TT8-T1*, (F-5′-tagaattcaatgcggctggaatat-3′ and R-5′-taaatttaattaatt caattagtatttg-3′)-*TT8-T2*, and (F-5′-catccaacgtctggtgaacc-3′ and R-5′- tcttagtgcttttgcaacatgtt-3′)-*TT8-T3* were used for *TT8*. Primer sequences (F-5′-cttcggaaaaactgaccggtt-3′ and R-5′-tttcatatccagagaatattccg-3′)-*PAP2-P1*, (F-5′-gtatttggttc gattcaaacatgc-3′ and R-5′-ggtcttttaatattattcgacaaa-3′)-*PAP2-P2*, and (F-5′-aaagtttttgtaagaaggtgcac-3′ and R-5′-tatatatatacacgt gaagggc-3′)-*PAP2-P3* were used for *PAP2*. Primer sequences (F-5′-acattcatgattccacaaattctaa-3′ and R-5′-ctttttcaaagtgagattggt tg-3′)-*MYBL2-M1* and (F-5′-ATGAACAAAACCCGCCTTCG-3′ and R-5′-GGGTCGATTCCCATTTTTACG-3′)-*MYBL2-CDS* were used for *MYBL2*. These experiments were repeated at least three times, with similar results.

In vitro pull-down assay

HIS-YDA, GST-EIN3, GST-CINV2, GST-SUC1, and GST-HXK1 expression constructs were prepared as described by Li *et al.* (2002). The potential for *in vitro* interaction between YDA and these GST fusion proteins was tested. Briefly, the HIS-YDA fusion and Ni-nitrilotriacetic acid sefinose resin (Sangon, Shanghai, China) were mixed at 4° for 2 hr of rocking, followed by brief centrifugation to precipitate beads and then washed three to four times with PBS buffer supplemented with 0.5% Tween 20. The precipitated beads were mixed with GST fusion protein or GST in the *in vitro* binding buffer (50 mM Tris-HCl, pH 7.5, 0.15 M NaCl, 1 mM DTT, 0.5% Triton X-100, and 1 mM phenylmethylsulfonyl fluoride) and incubated at 4° for 2 hr of rocking, followed by brief centrifugation to precipitate beads and then washed three to four times with PBS buffer supplemented with 0.5% Tween 20. The bound proteins were resolved by SDS-PAGE for immunoblot analysis using an anti-GST antibody. The reactive bands were visualized via exposure to nitroblue tetrazolium/bromochloroindolyl phosphate. These experiments were repeated at least four times, with similar results.

Co-immunoprecipitation analysis

Co-immunoprecipitation experiments using wild-type and transgenic plant extracts were performed according to Li *et al.* (2002) with minor modifications. Transgenic plants harboring both FLAG-EIN3 and GFP-YDA expression constructs were harvested. Soluble protein extracts were obtained using a protein extract kit (Sangon). Protein extracts were mixed with anti-FLAG M2 magnetic beads (Sigma, St. Louis, MO) and incubated at 4° overnight with gentle rocking, followed by brief centrifugation to precipitate beads and then washed three to four times with PBS buffer supplemented with 0.5% Tween 20. Co-immunoprecipitated GFP-YDA was screened by western analysis with anti-GFP (Sigma) antibodies. These experiments were repeated at least three times, with similar results.

Electrophoresis mobility shift assay

The electrophoresis mobility shift assay (EMSA) was performed using the LightShift Chemiluminescent EMSA Kit (20148; Pierce) according to the manufacturer's instructions. The biotin-labeled *TT8-T1* DNA fragments (5′-a**ttcaaa**aat

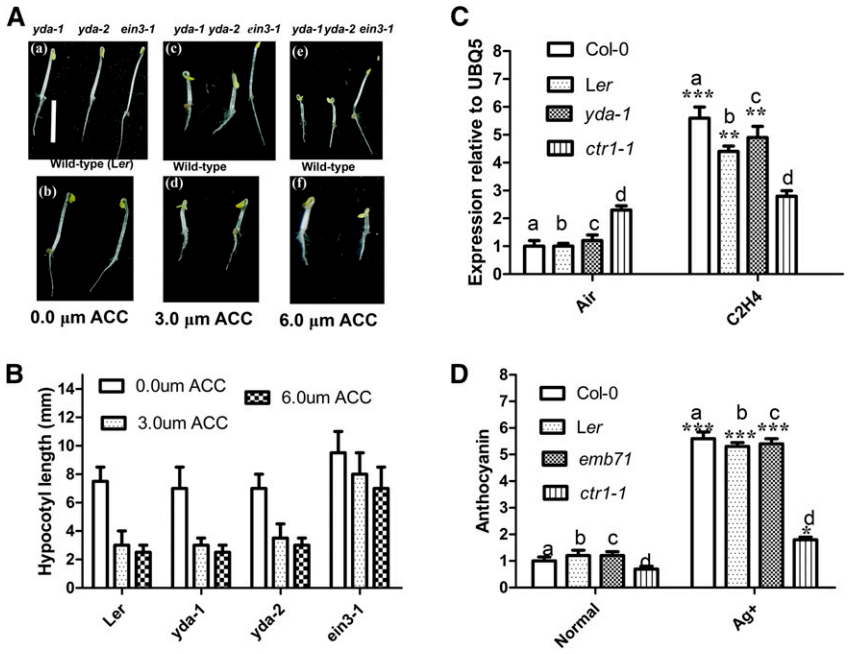

Figure 1 EMB71/YDA is not involved in ethylene signaling. (A) Representative 4-day-old *yda-1* (a), *yda-2* (a), *ein3-1* (a), and L*er* (b) seedlings grown on solid MS medium without ACC (1-aminocyclopropane-1-carboxylic acid); 4-day-old *yda-1* (c), *yda-2* (c), *ein3-1* (c), and L*er* (d) seedlings grown on solid MS medium with 3.0 m ACC; and 4-day-old *yda-1* (e), *yda-2* (e), *ein3-1* (e), and L*er* (f) seedlings grown on solid MS medium with 6.0 m ACC. Bar, 5.0 mm for a–f. (B) Bar graph exhibiting the difference in hypocotyl length between L*er*, *yda-1*, *yda-2*, and *ein3-1* seedlings grown on solid MS medium with 0.0 m ACC, 3.0 mACC, and 6.0 mACC, respectively. Error bars represent SD (n = 16). Experiments were repeated three times with similar results. (C) Bar graph exhibiting the difference of expression of *ERF1* between 8-day-old wild-type (Col-0), L*er*, *yda-1*, and *ctr1-1* light-grown seedlings with or without ethylene (25 ppm) for 5 hr. Data were from quantitative RT-PCR. Error bars indicate SD (n = 3; ** $P < 0.01$, *** $P < 0.001$). Value of wild-type seedlings without ethylene is set at 1.0. Quantifications were normalized to the expression of *UBQ5*. (D) Bar graph exhibiting the difference in anthocyanin accumulation between 10-day-old wild-type (Col-0), L*er*, *emb71*, and *ctr1-1* seedlings grown under white light. Wild-type value is set as 1.0. Error bars represent SD (n = 14; * $P < 0.05$, *** $P <$ 0.001). Experiments were repeated two times with similar results.

caaaagtcaacttttaatgcacttgagttttggtcatgcattcatatacatacatata-3′) and its mutated *PTT8-T1* DNA fragments (5′-a**ttctttt**aat caaaagtcaacttttaatgcacttgagttttggtcatgcattcatatacatacatata-3′), and the biotin-labeled *TT8-T2* DNA fragments (5′-aaca**ttcaaa** tataattagaggaccgtccaattggtatatgatcctactatattatttgggaagtacatt tt-3′) and its mutated *PTT8-T2* DNA fragments (5′-aaca**ttcttt** tataattagaggaccgtccaattggtatatgatcctactatattatttgggaagtacat ttt-3′) were synthesized, annealed, and used as probes. The corresponding biotin-unlabeled DNA fragments were utilized as competitor sequences in the assay. The probes were incubated with EIN3 fusion protein at room temperature for 20 min in a binding buffer [56 concentrations: 50 mM HEPES-KOH (pH 7.5), 375 mM KCl, 6.25 mM MgCl, 1 mM DTT, 0.5 mg/mL BSA, glycerol 25%]. Each 20 ml binding reaction contained 25 fmol Biotin-probe, 6 mg protein, and 1 mg poly(deoxyinosinic-deoxycytidylic) acid to minimize nonspecific interactions. The reaction products were analyzed by 6.5% native polyacrylamide gel electrophoresis. This experimental process has been described previously (Meng *et al.* 2015a,b).

Data availability

The authors affirm that all data necessary for confirming the conclusions of the article are present within the article and figures. Strains and/or plasmids are available upon request. Supplemental figures are available in supporting figures and legends file. Supplemental Material, File S1 shows that HXK1, SUC1, and CINV2 cannot directly interacts with YDA *in vitro*. File S2 shows that PAP2 and MYBL2 are not target genes of EIN3. All genomic data and genomic sequencing raw reads are available online at https://www.arabidopsis.org/. Supplemental material available at Figshare: https://doi.org/10.6084/m9.figshare.6974570.

Results

yda mutants are not defective in ethylene signaling

We recently reported that YDA can induce anthocyanin accumulation by regulating sucrose levels (Meng *et al.* 2016). Anthocyanin biosynthesis is negatively regulated through ethylene signaling and positively controlled through sugar signaling (Joeng *et al.* 2010). An antagonistic interaction between glucose and ethylene signaling has been widely observed (Yanagisawa *et al.* 2003). Given that YDA appears to regulate anthocyanin accumulation by a sugar signaling pathway, we explored if YDA might also regulate anthocyanin accumulation through ethylene function.

Using the methods of An *et al.* (2010), statistical analysis of hypocotyl and root growth showed that *yda* mutants produced both shortened hypocotyls and roots upon ACC treatment, similar to wild-type L*er* seedlings [Figure 1, A (a)–(f) and B]. Consistent with these phenotypes, the expression level of ethylene response gene *ERF1* was similar between wild-type and *yda-1* seedlings. However, the gene was expressed to high levels in the *constitutive triple response 1* (*ctr1*) mutant, which exhibited continuous ethylene signaling (Figure 1C). The inhibition of ethylene signaling by silver enhances the anthocyanin content of corn seedlings and wild-type *Arabidopsis* seedlings (Jeong *et al.* 2010). Treatment with silver resulted in significantly

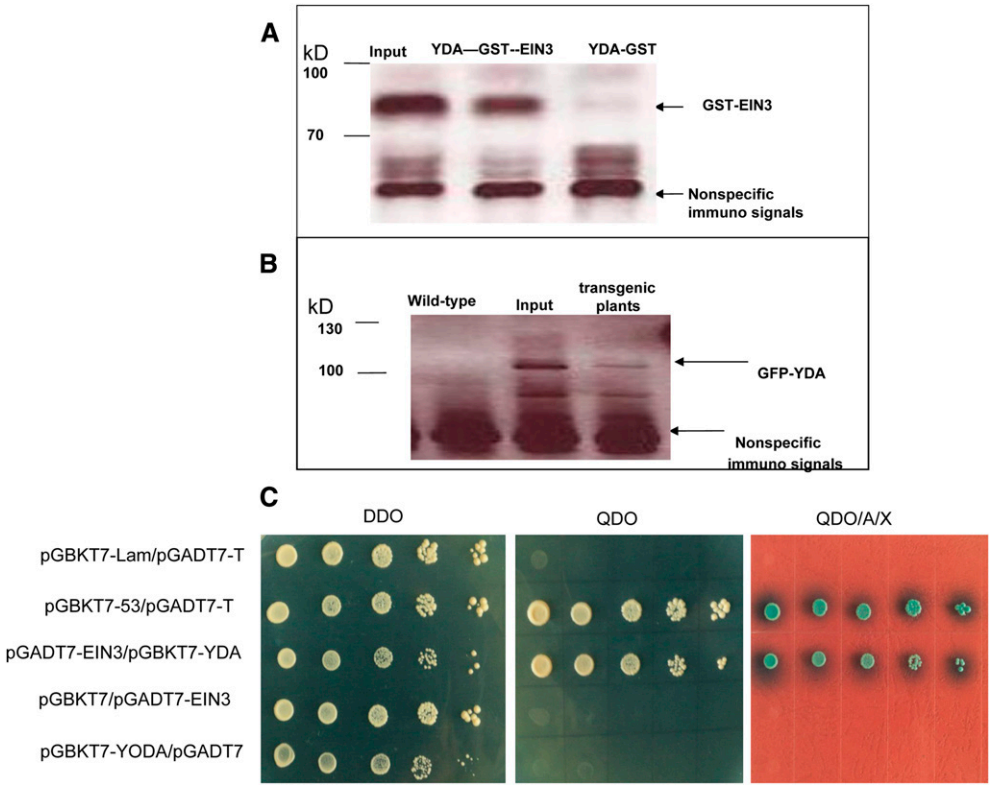

Figure 2 YDA interacts with EIN3. (A) HIS-YDA fusing protein exhibited specific affinity for GST-EIN3 but not GST *in vitro*. Input is considered as a positive control. (B) GFP-YDA showed specific affinity with FLAG-EIN3 *in vivo*. FLAG-EIN3 was associated with membranes and can be detected with anti-GFP antibodies. Wild type was used as a negative control. Input is considered as a positive control. (C) The cDNA of YODA and EIN3 were respectively inserted into pGBKT7 and pGADT7 to obtain the bait plasmid and the prey plasmids. Saccharomyces cerevisiae strain Y2H gold was cotransformed with pGBKT7-YODA and pGADT7-EIN3 vectors, and transformed Y2H Gold cells containing both vectors were selected using SD/-Leu-Trp(DDO), SD/-Leu-Trp-His-Ade(QDO), and SD/-Leu-Trp-His-Ade with X-α-gal and Aba(QDO/A/X). pGBKT7 and pGADT7 were bait and prey vectors without inserts. pGBKT7-53 and pGADT7-T encode two fusion proteins that are known to interact (Clontech). pGBKT7-Lam and pGADT7-T were used as negative controls. Serial dilutions of cotransformed yeast cells were used to measure the strength of the interaction.

enhanced anthocyanin accumulation in both wild-type and *yda* seedlings but not in *ctr1-1* seedlings (Figure 1D). Consistent with these findings, a previous study (Lukowitz *et al.* 2004) also proposed that *yda-1* and *yda-2* do not affect ethylene signaling. Taken together, our data suggested that YDA may not be required for ethylene function.

YDA interacts with EIN3 in vitro and in vivo

Key genes integral to sugar metabolism and/or signaling include *EIN3*, *HXOKINASE1* (*HXK1*), *SUCROSE-PROTON SYMPORTER1* (*SUC1*), and *CYTOSOLIC INVERTASE2* (*CINV2*) (Yanagisawa *et al.* 2003; Barratt *et al.* 2009). As YDA belongs to the MEKK1/Ste11/Bck1 class of MAPKKKs, which regulate protein targets by phosphorylation, YDA might regulate one or more of EIN3, HXK1, SUC1, and CINV2 at a post-translational level. To identify the potential target(s) of EMB71/YDA in the context of sugar signal transduction, we performed *in vitro* pull-down experiments. Full-length YDA was expressed as a HIS fusion protein, and full-length EIN3, HXK1, SUC1, and CINV2 were expressed as GST fusion proteins. Following mixing of the fusion proteins, sefinose resin was used to bind selectively to the HIS-YDA fusion protein. The potential presence of the coprecipitated GST fusion protein was examined using a GST antibody. Results indicated that YDA bound specifically to EIN3 *in vitro* (Figure 2A) but not to HXK1, SUC1, or CINV2 (Figure S1). Moreover, we performed *in vivo* co-immunoprecipitation experiments. Following transformation and associated genetic crosses, transgenic plants expressing both GFP-YDA and FLAG-EIN3 were produced. Subsequently, the total soluble protein in wild-type and FLAG-EIN3 transgenic seedlings was isolated, and an anti-FLAG antibody was utilized to potentially immunoprecipitate FLAG-EIN3. Potentially co-immunoprecipitated GFP-YDA was detected using a GFP antibody. Our data revealed a direct interaction between YDA and EIN3 *in planta* (Figure 2B). To confirm that YDA bound specifically to EIN3, we performed YH2 assay and BiFC. Our findings indicated that YDA could specifically interact with EIN3 (Figure 2C and Figure 3). Therefore, a YDA-EIN3 interaction may be relevant for the regulation of anthocyanin accumulation.

Increase in anthocyanin accumulation in ein3-1, eil1-3, and ein3/eil1 mutants is related to endogenous sucrose accumulation

Increased anthocyanin accumulation in *yda* mutants is closely related to enhanced endogenous sucrose accumulation (Meng *et al.* 2016), and YDA interacts with EIN3 *in vitro* and *in vivo* (Figure 2 and Figure 3). Therefore, whether the increase in anthocyanin accumulation in *ein3-1*, *eil1-3*, and *ein3/eil1* mutants is related to endogenous sucrose accumulation should be determined.

The *Arabidopsis* genome contains five EIN3 paralogs (EIL1–5). Among these paralogs, EIN3 and EIL1 are the most closely related. *EIL1* expression complements the *ein3* mutant

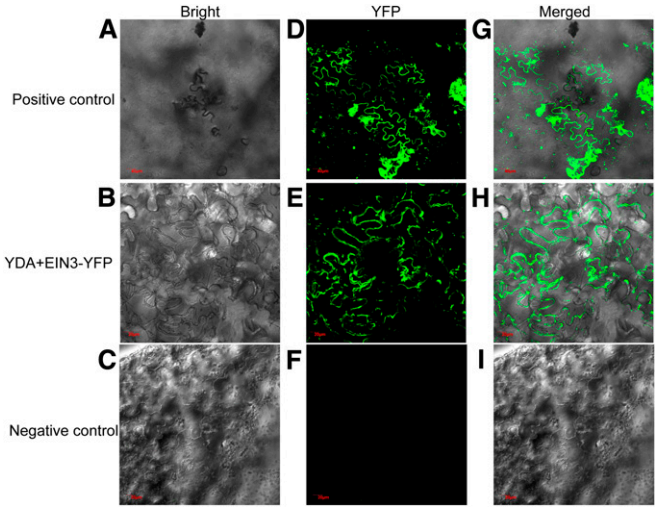

Figure 3 BiFC-based interactions between YDA and EIN3. Interactions with (A–C) bright, (D–F) YFP, and (G–I) merged. Pairs of proteins of YDA and EIN3 fused with halves of the YFP molecule were transiently expressed in wild tobacco leaves and reconstituted YFP fluorescence was imaged in epidermis on the abaxial leaf blades. Only EIN3 fused with halves of the YFP molecule was used as a negative control. Plasmid containing YFP was used as a positive control. Bar, 40 μm for A, D, and G; bar, 20.0 μm for B, C, E, F, H, and I.

and constitutively activates the ethylene response pathway (Chao *et al.* 1997). Thus, EIN3 and EIL1 appear redundant in biological function. When grown on solid MS medium supplemented with both 1% sucrose and 3% sucrose, no significant difference in anthocyanin accumulation was observed on the epidermis of the abaxial leaf surface between wild-type plants and the partial ethylene-insensitive mutants *ein3-1* and *eil1-3* (Figure 4, A and B). However, *ein3/eil1* plants presented increased anthocyanin accumulation compared with wild type, *ein3-1*, and *eil1-3* (Figure 4, A and B). Given that the endogenous sugar concentration can influence anthocyanin accumulation, we determined sucrose, glucose, and fructose levels in *ein3-1*, *eil1-3*, and *ein3/eil1* plants. Our findings indicated that the concentrations of sucrose and glucose, but not that of fructose, were significantly higher in *ein3-1*, *eil1-3*, and *ein3/eil1* than in wild-type seedlings (Figure 4, C–E).

When grown on solid MS medium supplemented with either 1 or 3% sucrose, increased anthocyanin accumulation was observed within the epidermis of the abaxial surface on *ein3/eil1* leaves relative to the corresponding organs in wild-type, *eil1-3*, and *ein3-1* seedlings (Figure 4, A and B). Anthocyanin biosynthesis is modulated by changes in Suc concentrations, and the sugar-dependent upregulation of the anthocyanin synthesis pathway is Suc-specific (Jeong *et al.* 2010). However, anthocyanin accumulation of *ein3/eil1* leaves was higher than that of *eil1-3* and *ein3-1* (Figure 4, A and B), whereas glucose and sucrose levels of *ein3/eil1* leaves were comparable with those of *eil1-3* and *ein3-1* (Figure 4, C–E). *eil1-3* and *ein3-1* are weak ethylene-insensitive mutants, and *ein3/eil1* is a strongly insensitive mutant; sugar-induced anthocyanin accumulation is inhibited by ethylene in *Arabidopsis* (Jeong *et al.* 2010). Therefore, ethylene signaling was more severely interrupted in *ein3/eil1* seedlings than in *eil1-3* and *ein3-1* seedlings. Although *ein3-1*, *eil1-3*, and *ein3/eil1* mutants exhibited similar increases in glucose and sucrose, only *ein3/eil1* mutants demonstrated increased anthocyanin levels. Collectively, the above findings indicated that the increase in anthocyanin accumulation in *ein3-1*, *eil1-3*, and *ein3/eil1* mutants was related to endogenous sucrose accumulation.

EIN3 negatively regulates TT8 via direct occupancy of its promoter

The above observations prompted us to examine whether EIN3 directly regulates the MBW transcription complex to control anthocyanin accumulation. Previous reports (Jeong *et al.* 2010) showed that expression levels of *DFR/TT3*, *TT18*, *TT8*, *UF3GT*, *PAP2*, and *MYLB2* are dramatically upregulated in *ein3-1* and *ein3/eil1* mutants relative to wild-type (Col-0) seedlings. We confirmed this result in the case of *TT8* by quantitative PCR (Figure 5A). We screened the promoters of these genes and found that their promoters' sequences all contained a putative EIN3 binding site (EBS; TACAT or TTCAAA; Figure 5B; Li *et al.* 2013). We then determined potential EIN3 binding to these promoters by ChIP-PCR analysis. Our findings indicated that EIN3 bound to the EBSs of the T1 and T2 regions of the *TT8* promoter (containing TTCAAA or TACAT sequences) and EBSs of the P2 region of the *miR164A* promoter when used as a positive control *in vivo* (Figure 5C; Li *et al.* 2013). By contrast, EIN3 could not bind to the EBSs of the T3 regions of the *TT8* promoter and wild-type, which were used as negative control (Figure 5C). Although the promoter sequences of *DFR/TT3*, *TT18*, *UF3GT*, *PAP2*, and *MYLB2* genes contained EBSs, EIN3 did not bind specifically to these promoter sequences (Figure S2). These results revealed that EIN3 did not bind to all EBSs. Thus, EIN3 binding to the promoter of *TT8 in vivo* might potentially require contributions from adjacent promoter sequences to support its binding specificity (Li *et al.* 2013). Additionally, EMSA experiments were performed to determine the *in vitro* binding of EIN3 to the *TT8-T1* and *TT8-2* EBS regions. Indeed, EIN3 could bind to the labeled *TT8-T1* and *TT8-2* elements *in vitro* (Figure 5D). Excessive unlabeled competitor DNA fragments effectively abolished this binding (Figure 5D). However, EIN3 was unable to bind mutant derivatives of EBSs from the *TT8-T1* and *TT8-2* regions of the cognate promoter (Figure 5E). Although the expression levels of *PAP2* and *MYBL2* were significantly enhanced in *ein3/eil1* seedlings, those of *TTG1*, *EGL3*, and *GL3* were not altered between *ein3/eil1* and wild-type seedlings (Jeong *et al.* 2010; Figure S2, A and B). Therefore, we focused on *PAP2* and *MYBL2*. However, our findings of ChIP-PCR indicated that EIN3 did not directly bind to the promoters of *PAP2* and *MYBL2* (Figure S2, C–F).

The *ein3/eil1* mutants showed higher anthocyanin accumulation than the control seedlings (12 days old), and the *tt8-1* mutant exhibited significantly less anthocyanin accumulation in comparison (Nesi *et al.* 2000; Joeng *et al.*

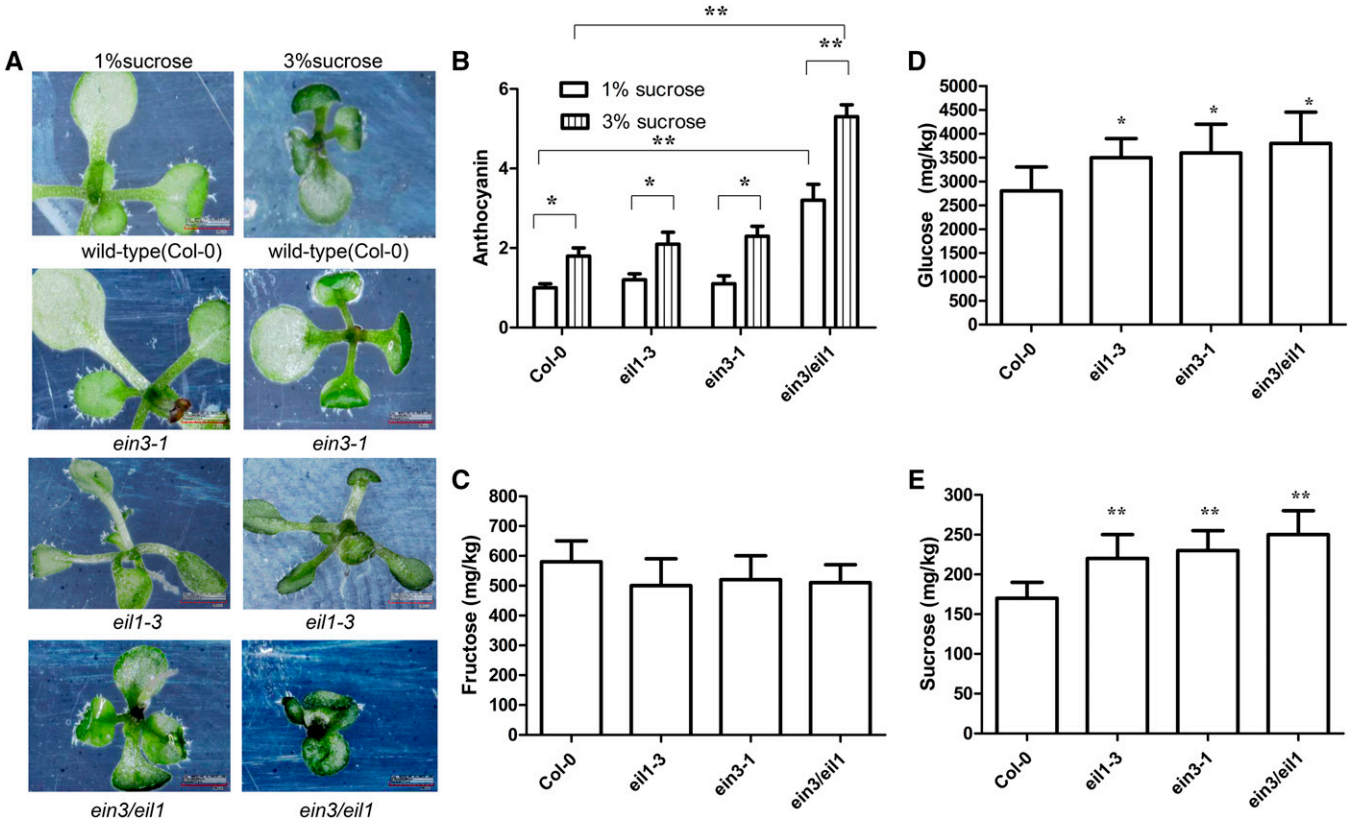

Figure 4 Alternation of anthocyanin accumulation in *ein3-1* and *ein3/eil1* mutants under abnormal endogenous sucrose accumulation. (A) Ten-day-old wild-type, *eil1-3*, *ein3-1*, and *ein3/eil1* seedlings grown under long light (16 hr light/8 hr dark) conditions on MS medium supplemented with 1% sucrose and 3% sucrose, respectively. Magnifications are the same. Seedlings were converted for showing abaxial side of leaves and then were photographed. (B) Bar graph exhibiting the difference in the anthocyanin accumulation under A. Col-0 is set as 1.0. Error bars represent SD (n = 3; ** $P < 0.01$). (C–E) Bar graphs exhibiting the different concentrations of hexose (glucose and fructose) (C and D) and sucrose (E) between wild-type (Col-0), *eil1-3*, *ein3-1*, and *ein3/eil1* seedlings grown under long light (16 hr light/8 hr dark) conditions on MS medium supplemented with 1% sucrose, respectively. Error bars represent SD (n = 3; * $P < 0.05$, ** $P < 0.01$).

2010; Figure 5F). Furthermore, *ein3/tt8* and *ein3/eil1/tt8* plants were found to have reduced anthocyanin accumulation relative to control seedlings (Figure 5F). Thus, loss of *TT8* function suppressed anthocyanin accumulation in the *ein3/eil1* double mutant. EIN3 acted genetically upstream of TT8, and EIN3/EIL1-TT8 formed a signaling cascade to regulate anthocyanin accumulation. Together, these findings indicated that *TT8* was a target of EIN3.

Discussion

YDA-EIN3-TT8 controls anthocyanin accumulation via protein–protein interactions

Although *yda-1* and *emb71* plants showed higher anthocyanin accumulation than control wild-type seedlings (Meng *et al.* 2016; Figure 6C), *ein3-1* mutants presented comparable anthocyanin accumulation with wild-type seedlings (Figure 4 and Figure 6C; Joeng *et al.* 2010). Furthermore, *yda/ein3* double-mutant seedlings presented comparable anthocyanin accumulation with wild-type and *ein3-1* seedlings (Figure 6C), suggesting that EIN3 was downstream of YDA, and loss of *EIN3* function significantly decreased anthocyanin content in *yda-1* mutants. These findings suggested a close relationship between YDA and EIN3 during anthocyanin accumulation. YDA interacted with EIN3, as proven by *in vitro* or *in vivo* pull-down assays, Y2H, and BiFC (Figure 2 and Figure 3). Influence of the absence of YDA function on endogenous sugar content (Figure 4; Meng *et al.* 2016) and specific sugar sensing, but not osmotic stress in general (Figure 6, A–C; Yanagisawa *et al.* 2003; Meng *et al.* 2016), provided additional support for possible regulatory activities of YDA upon EIN3. Moreover, EMB71/YDA-EIN3 directly targeted *TT8* by EIN3 (Figure 7), which may form an *EIN3-TT8* gene cascade for the regulation of anthocyanin accumulation. TT8 is a key regulator of anthocyanin and proanthocyanidin biosynthesis in *Arabidopsis* (Xu *et al.* 2013). Collectively, these data suggested that a YDA interaction with the EIN3-TT8 complex might regulate anthocyanin accumulation.

The precise mechanism by which YDA regulates EIN3 is presently unknown, but we found that YDA directly interacted with EIN3, which is a common target of both ethylene and sugar signaling (Yanagisawa *et al.* 2003). EIN3 contains an amino acid sequence motif reminiscent of a MAP kinase substrate docking domain (Sharrocks *et al.* 2000; Andreasson

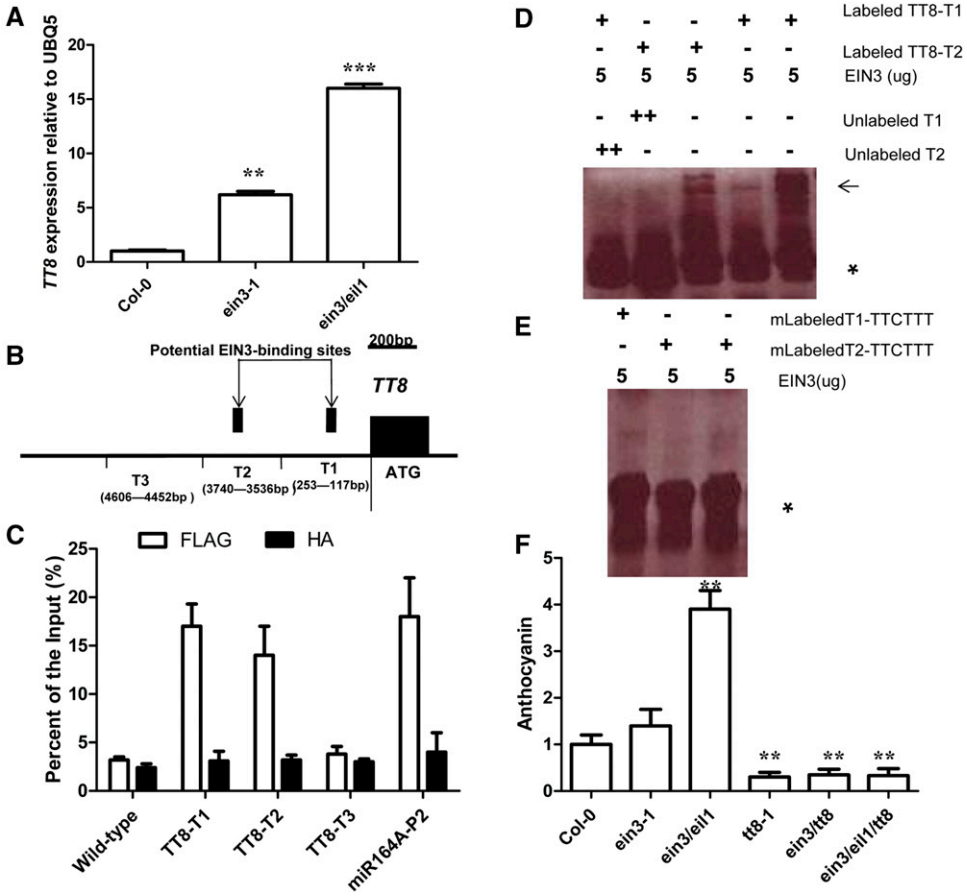

Figure 5 *TT8* is a target gene of EIN3. (A) Bar graph showing expression of *TT8* between Col-0, *ein3-1*, and *ein3/eil1* seedlings grown under white light conditions. Seedlings of at least five independently propagated lines were utilized. Wild-type data are set as 1.0. Quantification was normalized to the expression of *UBQ5*. Error bars represent SD (n = 4; ** $P < 0.01$, *** $P < 0.001$). (B) Schematic of the *TT8* promoter loci and their amplicons for ChIP analysis. (C) Chromatin immunoprecipitation (ChIP) analysis. Enrichment of particular *TT8* chromatin regions with anti-HA antibody (as a control) or anti-FLAG antibody in *EIN3-FLAG* transgenic plants and wild type as detected by real-time PCR analysis. Quantifications were normalized to the expression of *UBQ5*. Error bars represent SD (n = 4; ** $P < 0.01$). Input is set as 100% [supernatant including chromatin (input material) is considered as 100%, immunoprecipitated chromatin/input material × 100% for enrichment product of particular *TT8* chromatin regions]. P2 promoter of *miR164A* is a positive control, and the primers used for the P2 promoter have been described previously (Li *et al.* 2013). (D) Unlabeled *TT8* promoter (2.0 μg) was used as a competitor to determine the specificity of DNA-binding activity for EIN3. Free probe and EIN3 probe complexes are indicated by an asterisk and arrows, respectively. (E) A mutant version of the *TT8* promoter (AAA/TTT) was labeled with biotin and used for EMSA with EIN3 polypeptides. Free probe is indicated by an asterisk. (F) Bar graph showing the difference in anthocyanin accumulation between all indicated developmental seedling (12-day-old) grown under white light on solid MS medium with 1% sucrose. Col-0 data set as 1.0. Error bars represent SD (n = 10; ** $P < 0.01$). Experiments were repeated two times with similar results.

et al. 2005), which suggested that YDA might interact with EIN3 at this site. Given that YDA belongs to the MEKK1/Ste11/Bck1 class of MAPKKKs, EIN3 stability/function might be affected following YDA interaction and subsequent phosphorylation. The two proposed EIN3 phosphorylation sites are thought to show dual functions: T174 for stabilization and T592 for degradation (Yoo *et al.* 2008), but the kinase(s) responsible for EIN3 phosphorylation remain to be rigorously determined (Yoo *et al.* 2008; An *et al.* 2010).

Anthocyanin accumulation in yda mutants is positively correlated with sucrose accumulation

The anthocyanin biosynthetic pathway is strongly activated in response to increasing Suc concentrations, and this sugar-dependent upregulation is Suc-specific (Solfanelli *et al.* 2006; Jeong *et al.* 2010). In this work, we suggested that the increased sucrose concentration in *yda* seedlings might be responsible for anthocyanin accumulation. Although plant hormones such as auxin, ABA (Jeong *et al.* 2004; Hoth *et al.* 2010), cytokinin (Deikman and Hammer 1995), gibberellins (Weiss *et al.* 1995), and ethylene (Morgan and Drew 1997; Jeong *et al.* 2010) differentially regulate anthocyanin biosynthesis (Ozeki and Komamine 1986), *yda* did not affect signaling by these hormones (Lukowitz *et al.* 2004). Therefore, increased anthocyanin accumulation in *yda* mutants might predominantly result from a high endogenous sucrose concentration (Meng *et al.* 2016; Figure 6).

Proposed model for the regulation of anthocyanin biosynthesis

Increased anthocyanin accumulation was observed in the ethylene-insensitive mutants *etr1-1*, *ein2-1*, and *ein3/eil1*. By contrast, the constitutive ethylene-response mutant *ctr1-1*, partial ethylene-insensitive mutant *ein3-1*, and weak ethylene-insensitive mutant *eil1-3* exhibited comparable anthocyanin accumulation with wild-type seedlings (Jeong *et al.* 2010). These data were consistent with our results, which indicated that EIN3 and EIL1 were functionally redundant with respect to the regulation of anthocyanin accumulation. Thus, ethylene repressed the Suc-specific signaling pathway via the ethylene-mediated C2H4-Receptor-CTR1-EIN2-EIN3/EIL1-TT8 signaling cascade to regulate anthocyanin accumulation (Figure 7). Sugar and ethylene signaling were closely associated in the regulation of anthocyanin biosynthesis (Figure 7). Suc could enhance ethylene production in a dose-dependent manner in tobacco (Philosoph-Hadas *et al.* 1985), rice (*Oryza sativa*; Kobayashi and Saka

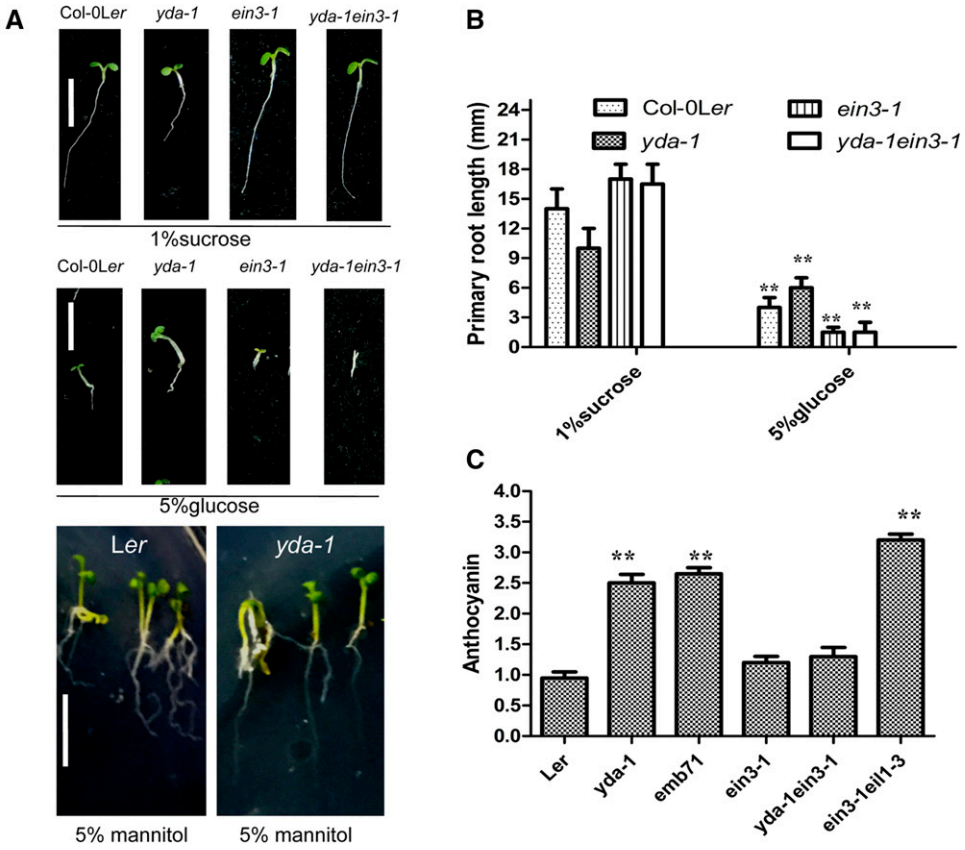

Figure 6 EIN3 mutation differentially suppresses *yda* mutant. (A) Representative 6-day-old seedlings grown on solid MS medium with 1% sucrose, 5% glucose, and 5% mannitol, and every kind of seedling have been indicated. Bar, 5 mm. (B) Bar graph exhibiting the difference in the root length between Col-0L*er*, *yda-1*, *ein3-1*, and *yda/ein3* seedlings grown on solid MS medium with 1% sucrose and 5% glucose, respectively. Error bars represent SD (n = 20; ** $P < 0.01$). Experiments were repeated two times with similar results. (C) Bar graph exhibiting the difference in the anthocyanin accumulation between the indicated seedlings grown under white light condition solid MS medium with 1% sucrose. Wild-type L*er* is set as 1.0. Error bars represent SD (n = 13; ** $P < 0.01$). Experiments were repeated two times with similar results.

2000), and *Arabidopsis* (Jeong *et al.* 2010) leaves. Meanwhile, ethylene modulates Suc and Glc sensitivity during *Arabidopsis* seedling development (Gibson *et al.* 2001).

In numerous cases, sucrose is not directly the signaling molecule, and many experiments have proven the role of hexose in triggering sugar signaling and responses in plants (Sheen *et al.* 1999). The role of hexose as signaling molecule but not substrate was also confirmed through the observation that hexokinase is a dimeric cytosolic enzyme essential for glycolysis (Sheen *et al.* 1999). Invertase (INV) controls plant growth and provides glucose for sucrose-dependent anthocyanin biosynthesis by catalyzing sucrose catabolism, which is one of the largest metabolic fluxes in plants (Barratt *et al.* 2009). *INV* gene expression levels are enhanced when the PAP1-related potato MYB transcription factor *Solanum tuberosum* anthocyanin 1 (*St*AN1) is infiltrated into tobacco leaves (Payyavula *et al.* 2013). Therefore, the YDA-EIN3 complex directly and negatively regulates the promoter of *TT8*, thereby influencing the MBW complex. MBW might in turn regulate INV activity, which degrades sucrose into fructose and glucose (Lou *et al.* 2007). Increased glucose levels promote YDA stability (Meng *et al.* 2016), which mediates the YDA-EIN3-TT8 pathway to regulate anthocyanin biosynthesis (Figure 7).

Whether YDA-EIN3 functions independently of MBW components is currently unknown. However, this relationship should be determined because many abiotic stresses induce anthocyanin biosynthesis as part of a coordinated nonspecific response to stress. In this work, building on a previous report (Jeong *et al.* 2010), we found that *TT8*, a member of MBW, was a target of EIN3. On the basis of quantitative PCR, ChIP-PCR, EMSA, and genetic analyses, our findings suggested that YDA-EIN3-TT8 formed a sugar signaling-mediated gene cascade that regulated anthocyanin biosynthesis (Figure 7). Moreover, microarray analysis of *pho3* plants, which are deficient in phosphorus and show high levels of anthocyanin accumulation, revealed an increased expression of *TT8* and genes encoding anthocyanin biosynthetic enzymes, implying that sugar was a trigger of anthocyanin biosynthesis *in vivo*.

Collectively, our findings enabled the synthesis of a model for the function of the EMB71/YDA-EIN3-EIL1-TT8 and C2H4-Receptor-CTR1-EIN2-EIN3/EIL1-TT8 signaling cascades in the regulation of anthocyanin biosynthesis. Suc signaling induces anthocyanin accumulation by the EMB71/YDA-EIN3-EIL1-TT8 signaling cascade and simultaneously induces ethylene production (Jeong *et al.* 2010). Ethylene subsequently mediates the suppression of anthocyanin accumulation by the C2H4-Receptor-CTR1-EIN2-EIN3/EIL1-TT8 signaling cascade (Figure 7). Thus, an antagonistic interaction exists between the EMB71/YDA-EIN3-EIL1-TT8 and C2H4-Receptor-CTR1-EIN2-EIN3/EIL1-TT8 signaling cascades. EIN3 is a common target of both ethylene and sugar signaling (Yoo *et al.* 2008). EIN3/EIL1 is a central component that coordinates either sugar or ethylene signaling, with opposing consequences for anthocyanin biosynthesis.

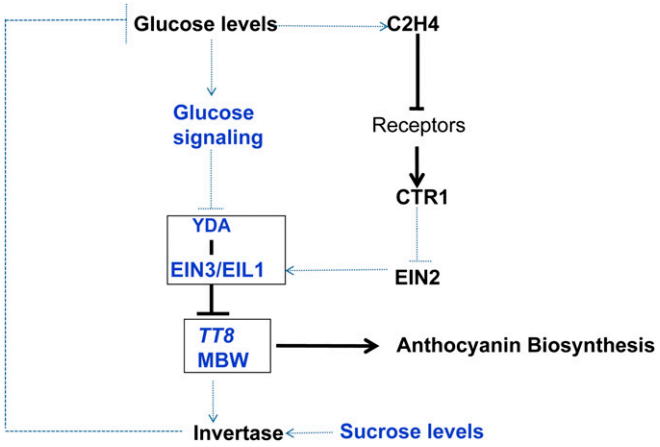

Figure 7 Model illustrating the regulation of anthocyanin biosynthesis by sugar and ethylene signaling. With exogenous sucrose supplied, increased sucrose levels may enhance invertase activity (Lou *et al.* 2007). Invertase can degrade sucrose into fructose and glucose, and generated glucose signaling/levels control YDA stability, which is due to glucose promoting YDA stability (Meng *et al.* 2016). And TT8, in turn, may control invertase activity by YDA-EIN3-TT8 signal transduction pathway (Payyavula *et al.* 2013). Thus, it appears to form a glucose signal loop for controlling sucrose-specifically depends on anthocyanin biosynthesis. This explains why anthocyanin biosynthesis specifically depends on sucrose. In a similar fashion, glucose signaling induces ethylene production, which also triggers the suppression of anthocyanin accumulation by the C2H4-Receptor-CTR1-EIN2-EIN3/EIL1 signal pathway. Solid lines indicate direct regulation, whereas dotted lines indicate either indirect regulation or regulation in an unknown manner.

Anthocyanins play a vital role in protecting plants against ultraviolet radiation, insect attack, and pathogen infection (Harborne and Williams 2000; Winkel-Shirley 2002; Gould 2004). However, the accumulation of anthocyanins above a threshold level is disadvantageous. For example, sustained anthocyanin accumulation can cause imbalances between primary and secondary metabolites (Jeong *et al.* 2010). Thus, plants may have evolved elaborate strategies to dynamically equilibrate anthocyanin biosynthesis within an effective but manageable range. Our findings suggested a molecular mechanism with multifaceted regulatory layers with which to finetune anthocyanin biosynthesis during plant growth and development.

Acknowledgments

We thank Gary. J. Loake (Edinburgh University) for kindly revising this manuscript. This work was funded by grants from the Natural Science Foundation of Jiangsu province of China (BK20170236) and the Postgraduate Research and Practice Innovation Program of Jiangsu Province (KYCX17-1614). The authors declare no competing financial interest.

Author contributions: L.-S.M. designed experiments. L.-S.M., M.-K.X., W.W., X.-Y.C., F.Y., Z.-Q.W., M.-J.L., C.L., and J.-Y.W. performed the experiments. L.-S.M. and M.-K.X. completed statistical analysis of data. L.-S.M., Z.-Y.L., and J.-H.J. wrote, edited, and revised this manuscript.

Literature Cited

An, F., Q. Zhao, Y. Ji, W. Li, Z. Jiang *et al.*, 2010 Ethylene-induced stabilization of ETHYLENE INSENSITIVE3 and EIN3-LIKE1 is mediated by proteasomal degradation of EIN3 binding F-box 1 and 2 that requires EIN2 in Arabidopsis. Plant Cell 22: 2384–2401. https://doi.org/10.1105/tpc.110.076588

Andreasson, E., T. Jenkins, P. Brodersen, S. Thorgrimsen, N. H. T. Petersen *et al.*, 2005 The MAP kinase substrate MKS1 is a regulator of plant defense responses. EMBO J. 24: 2579–2589. https://doi.org/10.1038/sj.emboj.7600737

Baier, M., G. Hemmann, R. Holman, F. Corke, R. Card *et al.*, 2004 Characterization of mutants in Arabidopsis showing increased sugar-specific gene expression, growth, and developmental responses. Plant Physiol. 134: 81–91. https://doi.org/10.1104/pp.103.031674

Barratt, D. H. P., P. Derbyshire, K. Findlay, M. Pike, N. Wellner *et al.*, 2009 Normal growth of Arabidopsis requires cytosolic invertase but not sucrose synthase. Proc. Natl. Acad. Sci. USA 106: 13124–13129. https://doi.org/10.1073/pnas.0900689106

Baudry, A., M. Caboche, and L. Lepiniec, 2006 TT8 controls its own expression in a feedback regulation involving TTG1 and homologous MYB and bHLH factors, allowing a strong and cell-specific accumulation of flavonoids in Arabidopsis thaliana. Plant J. 46: 768–779. https://doi.org/10.1111/j.1365-313X.2006.02733.x

Bemis, S. M., J. S. Lee, E. D. Shpak, and K. U. Torii, 2013 Regulation of floral patterning and organ identity by Arabidopsis ERECTA-family receptor kinase genes. J. Exp. Bot. 64: 5323–5333. https://doi.org/10.1093/jxb/ert270

Bergmann, D. C., W. Lukowitz, and C. R. Somerville, 2004 Stomatal development and pattern controlled by a MAPKK kinase. Science 304: 1494–1497. https://doi.org/10.1126/science.1096014

Borevitz, J. O., Y. Xia, J. Blount, R. A. Dixon, and C. Lamb, 2000 Activation tagging identifies a conserved MYB regulator of phenylpropanoid biosynthesis. Plant Cell 12: 2383–2394. https://doi.org/10.1105/tpc.12.12.2383

Chao, Q., M. Rothenberg, R. Solano, G. Roman, W. Terzaghi *et al.*, 1997 Activation of the ethylene gas response pathway in Arabidopsis by the nuclear protein ETHYLENE-INSENSITIVE3 and related proteins. Cell 89: 1133–1144. https://doi.org/10.1016/S0092-8674(00)80300-1

Deikman, J., and P. E. Hammer, 1995 Induction of anthocyanin accumulation by cytokinins in Arabidopsis thaliana. Plant Physiol. 108: 47–57. https://doi.org/10.1104/pp.108.1.47

Dooner, H. K., T. P. Robbins, and R. A. Jorgensen, 1991 Genetic and developmental control of anthocyanin biosynthesis. Annu. Rev. Genet. 25: 173–199. https://doi.org/10.1146/annurev.ge.25.120191.001133

Gibson, S. I., R. J. Laby, and D. Kim, 2001 The sugar-insensitive1 (sis1) mutant of Arabidopsis is allelic to ctr1. Biochem. Biophys. Res. Commun. 280: 196–203. https://doi.org/10.1006/bbrc.2000.4062

Gonzalez, A., M. Zhao, J. M. Leavitt, and A. M. Lloyd, 2008 Regulation of the anthocyanin biosynthetic pathway by the TTG1/bHLH/ Myb transcriptional complex in Arabidopsis seedlings. Plant J. 53: 814–827. https://doi.org/10.1111/j.1365-313X.2007.03373.x

Gould, K. S., 2004 Nature's swiss army knife: the diverse protective roles of anthocyanins in leaves. J. Biomed. Biotechnol. 2004: 314–320. https://doi.org/10.1155/S1110724304406147

Harborne, J. B., and C. A. Williams, 2000 Advances in flavonoid research since 1992. Phytochemistry 55: 481–504. https://doi.org/10.1016/S0031-9422(00)00235-1

Hoth, S., M. Niedermeier, A. Feuerstein, J. Hornig, and N. Sauer, 2010 An ABA responsive element in the AtSUC1 promoter is involved in the regulation of AtSUC1 expression. Planta 232: 911–923. https://doi.org/10.1007/s00425-010-1228-4

Jeong, S. T., N. Goto-Yamamot, S. Kobayashi, and M. Esaka, 2004 Effects of plant hormones and shading on the accumu-

lation of anthocyanins and the expression of anthocyanin biosynthetic genes in grape berry skins. Plant Sci. 167: 247–252. https://doi.org/10.1016/j.plantsci.2004.03.021

Jeong, S. W., P. K. Das, S. C. Jeoung, J. Y. Song, H. K. Lee *et al.*, 2010 Ethylene suppression of sugar-induced anthocyanin pigmentation in Arabidopsis. Plant Physiol. 154: 1514–1531. https://doi.org/10.1104/pp.110.161869

Kang, C. Y., H. L. Lian, F. F. Wang, J. R. Huang, and H. Q. Yang, 2009 Cryptochromes, phytochromes, and COP1 regulate light-controlled stomatal development in Arabidopsis. Plant Cell 21: 2624–2641. https://doi.org/10.1105/tpc.109.069765

Kobayashi, H., and H. Saka, 2000 Relationship between ethylene evolution and sucrose content in excised leaf blades of rice. Plant Prod. Sci. 3: 398–403. https://doi.org/10.1626/pps.3.398

Kubasek, W. L., B. W. Shirley, A. McKillop, H. M. Goodman, W. Briggs *et al.*, 1992 Regulation of flavonoid biosynthetic genes in germinating Arabidopsis seedlings. Plant Cell 4: 1229–1236. https://doi.org/10.1105/tpc.4.10.1229

Li, L., C. Ye, R. Zhao, X. Li, W.Z. Liu *et al.*, 2015 Mitogen-activated protein kinase kinase kinase (MAPKKK) 4 from rapeseed (Brassica napus L.) is a novel member inducing ROS accumulation and cell death.. Biochem. Biophys. Res. Commun. 467: 792–797. https://doi.org/10.1016/j.bbrc.2015.10.063

Li, J., J. Wen, K. A. Lease, J. T. Doke, F. E. Taxl *et al.*, 2002 BAK1, an Arabidopsis LRR receptor-like protein kinase, interacts with BRI and modulates brassinosteroid signaling. Cell 110: 213–222. https://doi.org/10.1016/S0092-8674(02)00812-7

Li, Z., J. Y. Peng, X. Wen, and H. W. Guo, 2013 ETHYLENE-INSENSITIVE3 is a senescence-associated gene that accelerates age-dependent leaf senescence by directly repressing miR164 transcription in Arabidopsis. Plant Cell 25: 3311–3328. https://doi.org/10.1105/tpc.113.113340

Lloyd, J. C., and O. V. Zakhleniuk, 2004 Responses of primary and secondary metabolism to sugar accumulation revealed by microarray expression analysis of the Arabidopsis mutant, pho3. J. Exp. Bot. 55: 1221–1230. https://doi.org/10.1093/jxb/erh143

Lou, Y., J. Y. Gou, and H. W. Xue, 2007 PIP5K9, an Arabidopsis phosphatidylinositol monophosphate kinase, interacts with a cytosolic invertase to negatively regulate sugar-mediated root growth. Plant Cell 19: 163–181. https://doi.org/10.1105/tpc.106.045658

Lukowitz, W., A. Roeder, D. Parmentr, and C. Somerville, 2004 A MAPKK kinase gene regulates extra-embryonic cell fate in Arabidopsis. Cell 116: 109–119. https://doi.org/10.1016/S0092-8674(03)01067-5

Meng, L. S., 2015 Transcription coactivator Arabidopsis ANGUSTIFOLIA3 modulates anthocyanin accumulation and light-induced root elongation through transrepression of constitutive Photomorphogenic1. Plant Cell Environ. 38: 838–851. https://doi.org/10.1111/pce.12456

Meng, L. S., and S. Q. Yao, 2015 Transcription co-activator Arabidopsis ANGUSTIFOLIA3 (AN3) regulates water-use efficiency and drought tolerance by modulating stomatal density and improving root architecture by the transrepression of YODA (YDA). Plant Biotechnol. J. 13: 893–902. https://doi.org/10.1111/pbi.12324

Meng, L. S., Y. B. Wang, S. Q. Yao, and A. Liu, 2015a Arabidopsis AINTEGUMENTA (ANT) mediates salt tolerance by transrepressing SCABP8. J. Cell Sci. 128: 2919–2927. https://doi.org/10.1242/jcs.172072

Meng, L. S., Z. B. Wang, S. Q. Yao, and A. Liu, 2015b The ARF2–ANT–COR15A gene cascade regulates ABA signaling-mediated resistance of large seeds to drought in Arabidopsis. J. Cell Sci. 128: 3922–3932. https://doi.org/10.1242/jcs.171207

Meng, L. S., Y. Q. Li, M. Q. Liu, and J. H. Jiang, 2016 The Arabidopsis ANGUSTIFOLIA3-YODA gene cascade induces anthocyanin accumulation by regulating sucrose levels. Front. Plant Sci. 7: 1728 [corrigenda: Front. Plant Sci. 8: 1228 (2017)]. https://doi.org/10.3389/fpls.2016.01728

Meng, L. S., C. Li, M. K. Xu, X. D. SUN, W. Wan *et al.*, 2018 Arabidopsis ANGUSTIFOLIA3 (AN3) is associated with the promoter of CONSTITUTIVE PHOTOMORPHOGENIC1 (COP1) to regulate light-mediated stomatal development. Plant Cell Environ. 41: 1645–1656. https://doi.org/10.1111/pce.13212

Morgan, P. W., and M. C. Drew, 1997 Ethylene and plant responses to stress. Physiol. Plant. 100: 620–630. https://doi.org/10.1111/j.1399-3054.1997.tb03068.x

Nesi, N., I. Debeaujon, C. Jond, G. Pelletier, M. Caboche *et al.*, 2000 The TT8 gene encodes a basic helix-loop-helix domain protein required for expression of DFR and BAN genes in Arabidopsis siliques. Plant Cell 12: 1863–1878. https://doi.org/10.1105/tpc.12.10.1863

Ozeki, Y., and A. Komamine, 1986 Effects of growth regulators on the induction of anthocyanin synthesis in carrot suspension cultures. Plant Cell Environ. 27: 1361–1368. https://doi.org/10.1093/oxfordjournals.pcp.a077234

Payne, C. T., F. Zhang, and A. M. Lloyd, 2000 GL3 encodes a bHLH protein that regulates trichome development in arabidopsis through interaction with GL1 and TTG1. Genetics 156: 1349–1362.

Payyavula, R. S., R. K. Singh, and D. A. Navarre, 2013 Transcription factors, sucrose, and sucrose metabolic genes interact to regulate potato phenylpropanoid metabolism. J. Exp. Bot. 64: 5115–5131. https://doi.org/10.1093/jxb/ert303

Philosoph-Hadas, S., S. Meir, and N. Aharoni, 1985 Carbohydrates stimulate ethylene production in tobacco leaf discs. II. Sites of stimulation in the ethylene biosynthesis pathway. Plant Physiol. 78: 139–143. https://doi.org/10.1104/pp.78.1.139

Qi, T. C., S. S. Song, Q. C. Ren, D. W. Wu, H. Huang *et al.*, 2011 The jasmonate-ZIM-domain proteins interact with the WD-repeat/bHLH/MYB complexes to regulate jasmonate-mediated anthocyanin accumulation and trichome initiation in Arabidopsis thaliana. Plant Cell 23: 1795–1814. https://doi.org/10.1105/tpc.111.083261

Rabino, I., and A. L. Mancinelli, 1986 Light, temperature, and anthocyanin production. Plant Physiol. 81: 922–924. https://doi.org/10.1104/pp.81.3.922

Rowan, D. D., M. Cao, K. Lin-Wang, J. M. Cooney, D. J. Jensen *et al.*, 2009 Environmental regulation of leaf colour in red 35S:PAP1 Arabidopsis thaliana. New Phytol. 182: 102–115. https://doi.org/10.1111/j.1469-8137.2008.02737.x

Sharrocks, A. D., S. H. Yang, and A. Galanis, 2000 Docking domains and substrate-specificity determination for MAP kinases. Trends Biochem. Sci. 25: 448–453. https://doi.org/10.1016/S0968-0004(00)01627-3

Sheen, J., L. Zhou, and J. C. Jang, 1999 Sugars as signaling molecules. Curr. Opin. Plant Biol. 2: 410–418.

Shirley, B. W., W. L. Kubasek, G. Storz, E. Bruggemann, M. Koornneef *et al.*, 1995 Analysis of Arabidopsis mutants deficient in flavonoid biosynthesis. Plant J. 8: 659–671. https://doi.org/10.1046/j.1365-313X.1995.08050659.x

Solfanelli, C., A. Poggi, E. Loreti, A. Alpi, and P. Perata, 2006 Sucrose-specific induction of the anthocyanin biosynthetic pathway in Arabidopsis. Plant Physiol. 140: 637–646. https://doi.org/10.1104/pp.105.072579

Stracke, R., M. Werber, and B. Weisshaar, 2001 The R2R3-MYB gene family in Arabidopsis thaliana. Curr. Opin. Plant Biol. 4: 447–456. https://doi.org/10.1016/S1369-5266(00)00199-0

Stracke, R., H. Ishihara, G. Huep, A. Barsch, F. Mehrtens *et al.*, 2007 Differential regulation of closely related R2R3-MYB transcription factors controls flavonol accumulation in different parts of the Arabidopsis thaliana seedling. Plant J. 50: 660–677. https://doi.org/10.1111/j.1365-313X.2007.03078.x

Teng, S., J. Keurentjes, L. Bentsink, M. Koornneef, and S. Smeekens, 2005 Sucrose-specific induction of anthocyanin biosynthesis in

Arabidopsis requires the MYB75/PAP1 gene. Plant Physiol. 139: 1840–1852. https://doi.org/10.1104/pp.105.066688

Toledo-Ortiz, G., E. Huq, and P. H. Quail, 2003 The Arabidopsis basic/helix-loop-helix transcription factor family. Plant Cell 15: 1749–1770. https://doi.org/10.1105/tpc.013839

Walker, A. R., P. A. Davison, A. C. Bolognesi-Winfield, C. M. James, N. Srinivasan *et al.*, 1999 The TRANSPARENT TESTA GLABRA1 locus, which regulates trichome differentiation and anthocyanin biosynthesis in Arabidopsis, encodes a WD40 repeat protein. Plant Cell 11: 1337–1350. https://doi.org/10.1105/tpc.11.7.1337

Weiss, D., A. Van Der Luit, E. Knegt, E. Vermeer, J. Mol *et al.*, 1995 Identification of endogenous gibberellins in petunia flowers (induction of anthocyanin biosynthetic gene expression and the antagonistic effect of abscisic acid). Plant Physiol. 107: 695–702. https://doi.org/10.1104/pp.107.3.695

Winkel-Shirley, B., 2001 Flavonoid biosynthesis. A colorful model for genetics, biochemistry, cell biology, and biotechnology. Plant Physiol. 126: 485–493. https://doi.org/10.1104/pp.126.2.485

Winkel-Shirley, B., 2002 Biosynthesis of flavonoids and effects of stress. Curr. Opin. Plant Biol. 5: 218–223. https://doi.org/10.1016/S1369-5266(02)00256-X

Xu, W., D. Grain, J. Le Gourrierec, E. Harscoët, A. Berger *et al.*, 2013 Regulation of flavonoid biosynthesis involves an unexpected complex transcriptional regulation of TT8 expression, in Arabidopsis. New Phytol. 198: 59–70. https://doi.org/10.1111/nph.12142

Yanagisawa, S., S. D. Yoo, and J. Sheen, 2003 Differential regulation of EIN3 stability by glucose and ethylene signalling in plants. Nature 425: 521–525. https://doi.org/10.1038/nature01984

Yoo, S. D., Y. H. Cho, G. Tena, Y. Xiong, and J. Sheen, 2008 Dual control of nuclear EIN3 by bifurcate MAPK cascades in C_2H_4 signalling. Nature 451: 789–795. https://doi.org/10.1038/nature06543

Zhang, F., A. Gonzalez, M. Zhao, C. T. Payne, and A. Lloyd, 2003 A network of redundant bHLH proteins functions in all TTG1-dependent pathways of Arabidopsis. Development 130: 4859–4869. https://doi.org/10.1242/dev.00681

Zimmermann, I. M., M. A. Heim, B. Weisshaar, and J. F. Uhrig, 2004 Comprehensive identification of Arabidopsis thaliana MYB transcription factors interacting with R/B-like BHLH proteins. Plant J. 40: 22–34. https://doi.org/10.1111/j.1365-313X.2004.02183.x

Communicating editor: N. Springer